Implementation of Finite Control Set Model Predictive Control (FCS-MPC) for Five-Phase Induction Motors

Abdelfattah Hoggui, Ali Benachour, Mohamed Chafaa Madaoui, and Mohand Oulhadj Mahmoudi

Abstract—This paper investigates the study and practical implementation of Finite Control Set Model Predictive Control (FCS-MPC) for a five-phase induction motor powered by a two-level, five-phase voltage source inverter. Multiphase systems present notable benefits over conventional three-phase configurations, including improved fault tolerance, enhanced torque production, and minimized harmonic distortion, making them well-suited for demanding applications. FCS-MPC operates by directly predicting and selecting the optimal control action at each sampling instant, eliminating the necessity of a modulation stage and offering fast dynamic response. The proposed control approach is designed and validated through experimental testing, assessing key performance indicators such as speed tracking, torque ripple, and current distortion under both transient and steady-state conditions. The experimental results demonstrate the effectiveness of FCS-MPC in ensuring precise and efficient control across various operating scenarios, making it a viable alternative for multiphase motor drive applications.

***Keywords*—five-phase induction motor, two-level five-phase voltage source inverter, finite control set model predictive control (FCS-MPC).**

I. Introduction

In recent years, multiphase motor systems have gained increasing attention due to their potential for enhanced performance, reliability, and efficiency in various industrial applications. Among these, five-phase induction motors have emerged as a viable alternative to conventional three-phase machines, offering key advantages such as improved fault tolerance, reduced torque ripple, and lower harmonic distortion. These characteristics make five-phase systems particularly suitable for demanding applications, including renewable energy generation, electric transportation, and high-precision industrial drives [1–6].

The unique benefits of five-phase induction motors have driven researchers to extend and adapt control strategies originally developed for three-phase systems to these advanced multiphase configurations [7–20]. One such technique is Finite Control Set Model Predictive Control (FCS-MPC), which has gained prominence as an alternative to conventional control methods due to its ability to directly predict and optimize switching states at each sampling interval [21–25].

FCS-MPC is based on a predictive control that utilizes the mathematical model of the system to estimate future states and minimize a predefined cost function. This approach allows direct control of stator currents, torque, and flux without requiring coordinate transformations or pulse-width modulation (PWM). By continuously evaluating the impact of different switching states, FCS-MPC ensures fast dynamic response, improved transient performance, and precise control of electromagnetic variables, making it an attractive solution for multiphase motor drives.

This paper is structured as follows: Section II presents the modeling of the five-phase induction motor, followed by the mathematical formulation of the two-level five-phase voltage source inverter. Section III introduces the principles of FCS-MPC and its application to five-phase motor control. In Section IV, experimental results are analyzed to evaluate the performance of FCS-MPC under various operating conditions. Finally, Section V concludes the paper with key findings and potential research directions.

II. Modeling of the Five-Phase Induction Machine

The mathematical representation of five-phase induction machines is derived from their distinct winding configuration and electromagnetic characteristics. To simplify the modeling process, the following assumptions are considered in this work [13]:

- The magnetic circuit operates within a linear region, neglecting saturation effects and assuming constant permeability.
- The magnetomotive force (MMF) distribution and the resulting air-gap flux are considered sinusoidal.
- Hysteresis, eddy current losses, and skin effect are disregarded, focusing the model solely on electromagnetic interactions.

Manuscript received March 6, 2025; revised June 15, 2025.

A. Hoggui, M.C. Madaoui and M.O. Mahmoudi are with the Laboratoire de Recherche en Electrotechnique (LRE), Ecole Nationale Poly-technique (ENP), B.P. 182 El Harrach, Algiers 16200, Algeria.e-mail: (abdelfettah.hoggui@g.enp.edu.dz).

A. Benachour is with the Electrical Engineering Department, Ecole Nationale Supérieure des Technologies Avancées, Algiers, ALGERIA. e-mail: (ali.benachour@ensta.edu.dz).

Digital Object Identifier (DOI): 10.53907/enpesj.v5i1.325

- A uniform air-gap thickness is assumed to facilitate the magnetic circuit analysis.

Five-phase induction motors have five stator windings that are symmetrically arranged with a spatial displacement of $\frac{2\pi}{5}$. The corresponding arrangement is shown in Fig. 1

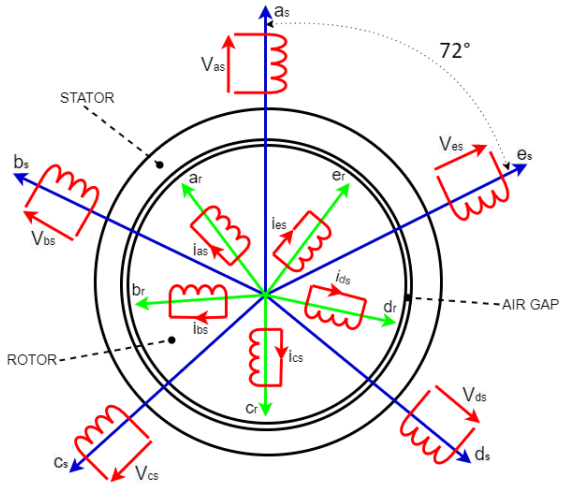

Fig. 1: Winding arrangement of a five-phase induction machine.

The equations describing the voltage and flux linkage for the stator and rotor phases are presented as follows:

$$\begin{cases} \mathbf{V}_s = \mathbf{R}_s\mathbf{I}_s + \dfrac{d}{dt}\mathbf{\Phi}_s, \\ \mathbf{\Phi}_s = \mathbf{L}_s\mathbf{I}_s + \mathbf{L}_{sr}\mathbf{I}_r, \end{cases} \tag{1}$$

$$\begin{cases} \mathbf{V}_r = \mathbf{R}_r\mathbf{I}_r + \dfrac{d}{dt}\mathbf{\Phi}_r - j\omega_r\mathbf{\Phi}_r, \\ \mathbf{\Phi}_r = \mathbf{L}_r\mathbf{I}_r + \mathbf{L}_{rs}\mathbf{I}_s, \end{cases} \tag{2}$$

where:

- $\mathbf{V}_s$ and $\mathbf{V}_r$ are the stator and rotor voltages,
- $\mathbf{I}_s$ and $\mathbf{I}_r$ are the stator and rotor currents,
- $\mathbf{\Phi}_s$ and $\mathbf{\Phi}_r$ represent the stator and rotor flux linkages,
- $\mathbf{R}_s$, $\mathbf{R}_r$, $\mathbf{L}_s$, $\mathbf{L}_r$, $\mathbf{L}_{sr}$, and $\mathbf{L}_{rs}$ are the stator and rotor resistances, self-inductances, and mutual inductances,
- ω_r is the rotor speed.

While these equations provide an accurate representation of the machine in the natural $(a-b-c-d-e)$ coordinate system, the presence of time-varying coefficients complicates their use in control applications. To facilitate implementation, the stator and rotor equations are transformed into the $(\alpha-\beta-x-y-z)$ reference frame using Park's transformation. This transformation simplifies the control structure by decoupling the torque-producing $(\alpha-\beta)$ components from the $(x-y-z)$ components, which do not contribute to electromagnetic torque production. The resulting equations in the transformed domain are given by:

$$\begin{cases} V_{\alpha s} = R_s I_{\alpha s} + \dfrac{d\Phi_{\alpha s}}{dt} - \omega\Phi_{\beta s}, \\ V_{\beta s} = R_s I_{\beta s} + \dfrac{d\Phi_{\beta s}}{dt} + \omega\Phi_{\alpha s}, \end{cases} \tag{3}$$

The electromagnetic torque generated by the five-phase induction machine is expressed as:

$$T_e = \frac{5}{2}p\left(\Phi_{\alpha s}I_{\beta s} - \Phi_{\beta s}I_{\alpha s}\right), \tag{4}$$

where:

- T_e represents the electromagnetic torque,
- p denotes the number of pole pairs,
- $\Phi_{\alpha s}$ and $\Phi_{\beta s}$ are the α-β axis flux components,
- $I_{\alpha s}$ and $I_{\beta s}$ correspond to the α-β axis current components.

This model serves as a foundation for implementing advanced control strategies suitable for five-phase machines. By focusing on the torque-generating α-β components, the effects of the non-torque-producing $(x-y-z)$ components are disregarded. Although these additional components may introduce extra losses in the machine [9, 14–17], studies have shown that their impact is negligible in practical applications. Therefore, for the sake of simplicity, these losses are not considered in this work. The developed model provides a structured framework for implementing predictive control techniques, particularly FCS-MPC, which relies on the discrete-time representation of system dynamics to optimize control performance.

III. Two-Level Five-Phase Inverter

Fig. 2 presents the topology of a two-level five-phase inverter, which serves as the power source for the stator windings of the five-phase induction motor considered in this paper.

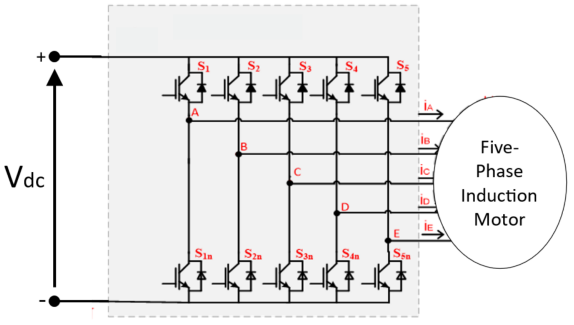

Fig. 2: Topology of the two-level five-phase inverter.

The inverter is composed of five legs, each incorporating two insulated-gate bipolar transistors (IGBTs) operating in a complementary switching scheme. This configuration results in 32 distinct switching states. Each switching state corresponds to a specific space voltage vector, forming a set that includes two zero vectors and thirty active vectors with different magnitudes. The spatial distribution of these voltage vectors in the $\alpha-\beta$ plane is depicted in Fig. 3.

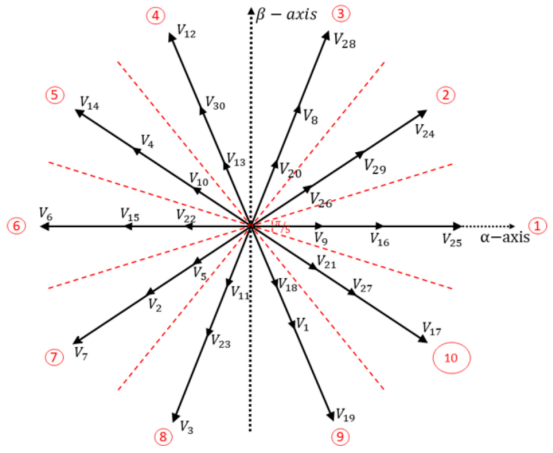

Fig. 3: Space voltage vector of the two-level five-phase inverter in the $\alpha - \beta$ plane.

IV. Finite Control Set Model Predictive Control for a Five-Phase Induction Motor

Fig. 4 presents the schematic representation of the FCS-MPC applied to a five-phase induction motor. It outlines the main components of the control loop, including the predictive model, cost function evaluation, and selection of the optimal switching states.

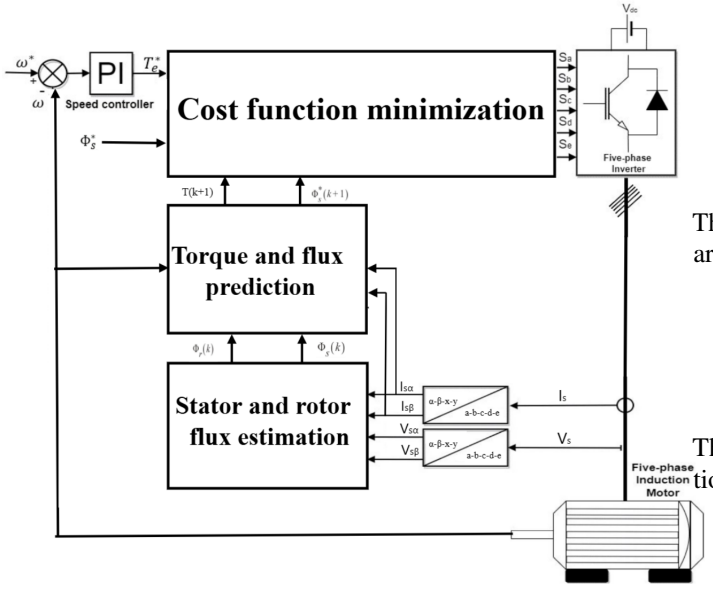

Fig. 4: Schematic diagram of the FCS-MPC control strategy.

For five-phase induction motor control, FCS-MPC employs a predictive approach based on the motor's mathematical model in the stationary reference frame. The controller forecasts future states, such as stator currents and both stator and rotor flux linkages, by considering different inverter switching states. The predictive process relies on discretizing the motor's dynamic equations and using these discrete models to estimate system behavior over a short prediction horizon. At each sampling step, the controller evaluates all possible voltage vectors (corresponding to the five-phase inverter's switching states) and calculates a cost function that includes terms for tracking errors [18].

The continuous-time model defined in system (3), expressed in a reference frame rotating at an arbitrary speed ω, is transformed into the stationary (α-β-x-y-o) reference frame. For implementation in a digital controller, the system is then discretized using a sampling period T_s. To simplify computations, only the torque-producing α-β components are considered in this work. The discrete-time expressions for the stator flux linkages are formulated as follows:

$$\begin{aligned}\Phi_{s\alpha}[k+1] &= \Phi_{s\alpha}[k] + T_s\left(V_{s\alpha}[k] - R_s I_{s\alpha}[k]\right)\\ \Phi_{s\beta}[k+1] &= \Phi_{s\beta}[k] + T_s\left(V_{s\beta}[k] - R_s I_{s\beta}[k]\right)\end{aligned} \tag{5}$$

Similarly, the rotor flux linkage equations in discrete form are given by:

$$\begin{aligned}\Phi_{r\alpha}[k+1] &= \left(1 - \frac{R_r T_s}{L_r}\right)\Phi_{r\alpha}[k] + T_s\omega_m\Phi_{r\beta}[k]\\ &\quad + \frac{R_r T_s L_m}{L_r} I_{s\alpha}[k]\\ \Phi_{r\beta}[k+1] &= \left(1 - \frac{R_r T_s}{L_r}\right)\Phi_{r\beta}[k] - T_s\omega_m\Phi_{r\alpha}[k]\\ &\quad + \frac{R_r T_s L_m}{L_r} I_{s\beta}[k]\end{aligned} \tag{6}$$

The rotor currents can be expressed in terms of the rotor flux linkages as:

$$\begin{aligned}I_{r\alpha}[k+1] &= \frac{\Phi_{r\alpha}[k+1] - L_m I_{s\alpha}[k+1]}{L_r}\\ I_{r\beta}[k+1] &= \frac{\Phi_{r\beta}[k+1] - L_m I_{s\beta}[k+1]}{L_r}\end{aligned} \tag{7}$$

The stator flux linkages in relation to the stator and rotor currents are expressed as:

$$\begin{aligned}\Phi_{s\alpha}[k+1] &= L_s I_{s\alpha}[k+1] + L_m I_{r\alpha}[k+1]\\ \Phi_{s\beta}[k+1] &= L_s I_{s\beta}[k+1] + L_m I_{r\beta}[k+1]\end{aligned} \tag{8}$$

The stator currents are then updated using the following relations:

$$X_\alpha[k] = \frac{1}{R_\sigma}\left(\frac{k_r}{\tau_r}\Phi_{r\alpha}[k] + k_r\omega_m\Phi_{r\beta}[k]\right)$$

$$X_\beta[k] = \frac{1}{R_\sigma}\left(\frac{k_r}{\tau_r}\Phi_{r\beta}[k] - k_r\omega_m\Phi_{r\alpha}[k]\right)$$

$$\begin{aligned}I_{s\alpha}[k+1] &= \left(1 + \frac{T_s}{\tau_\sigma}\right)I_{s\alpha}[k] + \frac{T_s}{\tau_\sigma}\left(X_\alpha[k] + V_{s\alpha}[k]\right)\\ I_{s\beta}[k+1] &= \left(1 + \frac{T_s}{\tau_\sigma}\right)I_{s\beta}[k] + \frac{T_s}{\tau_\sigma}\left(X_\beta[k] + V_{s\beta}[k]\right)\end{aligned} \tag{9}$$

where:

- $\sigma = 1 - \frac{L_m^2}{L_r L_s}$

- $\tau_\sigma = \frac{\sigma L_s}{R_\sigma}$
- $k_r = \frac{L_m}{L_r}$
- $\tau_r = \frac{L_r}{R_r}$
- $R_\sigma = R_s + k_r^2 R_r$
- ω_m is the mechanical angular velocity.

The predicted electromagnetic torque at the next time step is computed using:

$$T_e[k+1] = \frac{5}{2} p \left(\Phi_{s\alpha}[k+1] I_{s\beta}[k+1] - \Phi_{s\beta}[k+1] I_{s\alpha}[k+1]\right) \tag{10}$$

To achieve precise control of the motor, the cost function in this study aims to minimize errors in torque and stator flux, formulated as:

$$J = \lambda_T \left|T_e[k+1] - T_{\text{ref}}\right| + \lambda_\Phi \left|\Phi_s[k+1] - \Phi_{s,\text{ref}}\right| \tag{11}$$

where:

- λ_T and λ_Φ are weighting factors for torque and flux errors, respectively.
- $T_e[k+1]$ is the predicted electromagnetic torque at the next time step.
- T_{ref} is the reference torque.
- $\Phi_s[k+1]$ is the predicted stator flux magnitude.
- $\Phi_{s,\text{ref}}$ is the reference stator flux magnitude.

The control algorithm evaluates all 32 possible switching states and selects the one that minimizes the cost function. This optimization ensures minimal tracking error and efficient control.

V. EXPERIMENTAL RESULTS

Fig. 5 illustrates the experimental test bench utilized for implementing the Finite Control Set Model Predictive Control (FCS-MPC) strategy on a five-phase induction motor. The setup consists of a transformer supplying a rectifier, which delivers a DC voltage. This DC voltage powers two two-level three-phase inverters configured to supply the five-phase induction motor.

The five-phase induction motor is mechanically coupled to a DC generator, which serves as the load. The load level can be adjusted using a variable resistor connected to the DC generator, enabling precise control of the operating conditions.

The FCS-MPC control algorithm is implemented on a dSPACE 1104 control board, which interfaces with the system for real-time control and data acquisition. A current measurement circuit is integrated into the setup. Additionally, an incremental encoder

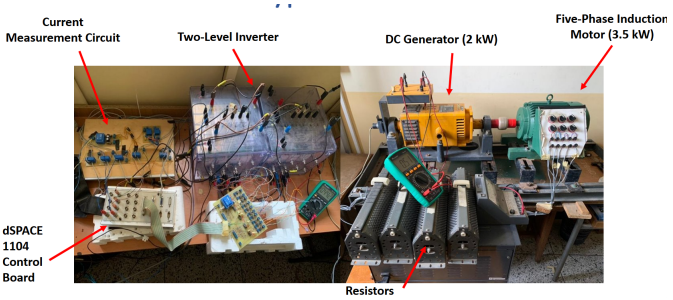

Fig. 5: Experimental test bench used for FCS-MPC implementation.

is used to measure the motor's rotational speed, providing essential data for the closed-loop control system. The parameters of the five-phase induction motor used in this setup are presented in a table in the appendix.

To evaluate the performance of the FCS-MPC strategy applied to the five-phase induction motor, two experimental tests were conducted under varying speed conditions while maintaining a constant load. In the first test, the reference speed was incremented from 50 rad/s to 200 rad/s in steps of 50 rad/s and subsequently reduced from 200 rad/s to 150 rad/s under the same load conditions. In the second test, the reference speed was varied to assess the system's performance during speed reversals: it started at 50 rad/s, increased to 100 rad/s, and then decreased to –150 rad/s in steps of 50 rad/s.

The results, presented in Fig. 6 and Fig. 7, provide insight into key electromagnetic parameters, including the reference and actual speed, the electromagnetic torque and its reference, as well as the flux magnitude and its reference.

Fig. 6(a) and Fig. 7(a) show that the rotor speed closely follows its reference, with minimal overshoot during acceleration and deceleration. The motor smoothly transitions between speed levels, highlighting the capability of the FCS-MPC strategy in ensuring fast and precise speed adjustments.

Fig. 6(b) and Fig. 7(b) shows that the electromagnetic torque closely follows its reference, with minimal ripple in both forward and reverse rotational directions. In steady-state operation, the torque ripple varies depending on the reference speed.

Fig. 6(c) and Fig. 7(c) illustrate that the path of the stator flux forms an almost perfect circle, demonstrating that it has a consistent magnitude with minimal ripple in both forward and reverse rotational directions, as confirmed in Fig. 6(d) and Fig. 7(d).

Fig. 8 illustrates the electrical performance of the FCS-MPC strategy at constant speed. It presents the inverter's output voltage along with its harmonic spectrum, as well as the stator current and its corresponding harmonic spectrum.

The results show that the total harmonic distortion (THD) of the inverter's output voltage is notably high due to the variable switching frequency of the FCS-MPC strategy. On the other hand, the stator current THD is significantly lower, benefiting from the filtering effect of high-frequency harmonics, a characteristic effect of the inductive properties of the induction machine. Additionally, during speed variations, peak current values reach 5A.

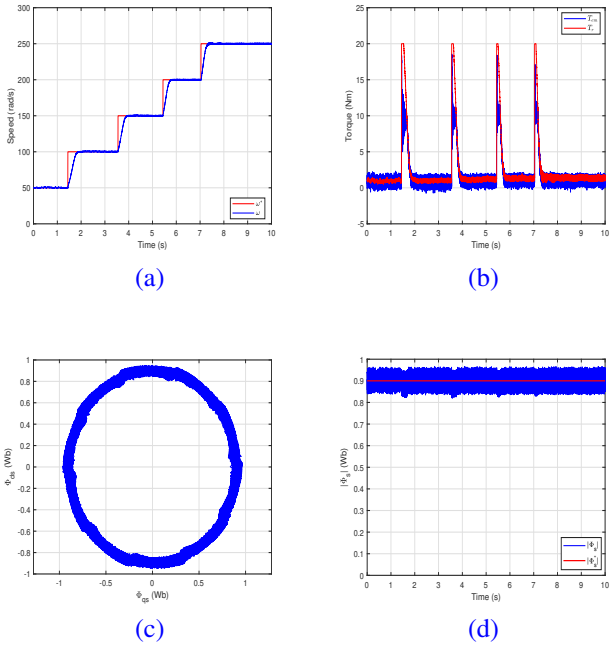

Fig. 6: Experimental results of FCS-MPC: (a) Rotor speed and reference speed, (b) Electromagnetic torque and reference torque, (c) Stator flux trajectory, and (d) Stator flux magnitude with its reference.

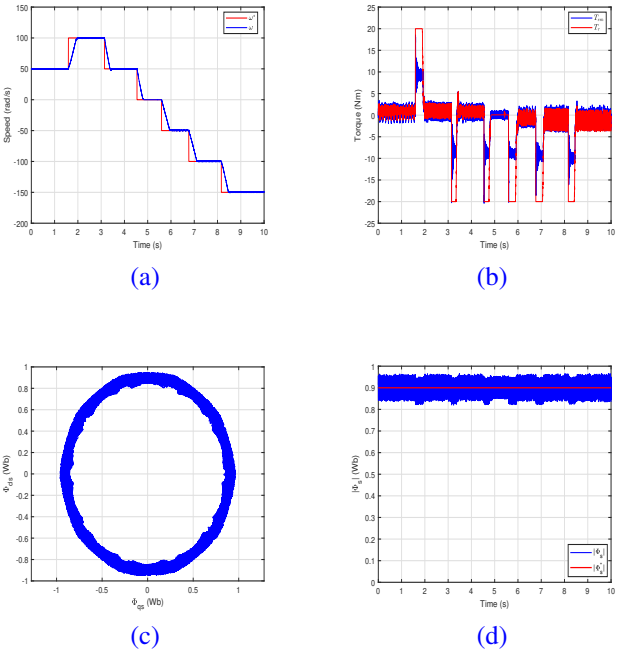

Fig. 7: Experimental results of FCS-MPC : (a) Rotor speed and reference speed, (b) Electromagnetic torque and reference torque, (c) Stator flux trajectory, and (d) Stator flux magnitude with its reference.

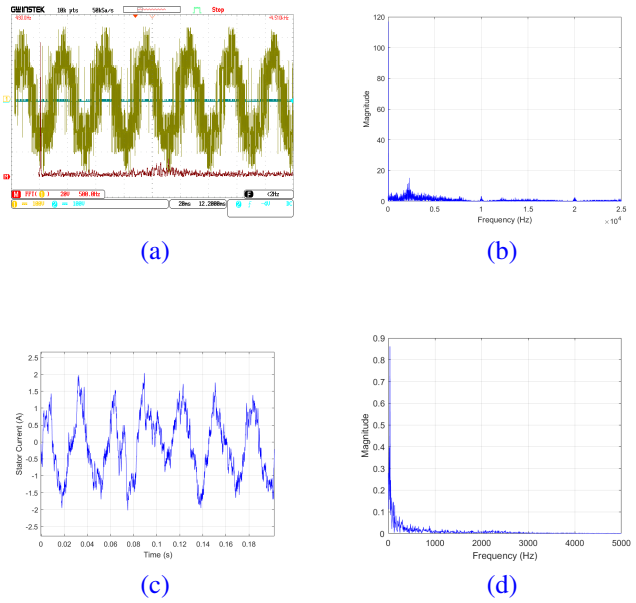

Fig. 8: Experimental results of FCS-MPC: (a) Inverter output voltage, (b) Harmonic spectrum of the inverter output voltage, (c) Stator currents, and (d) Harmonic spectrum of stator currents.

VI. Conclusion

This paper demonstrates that the Finite Control Set Model Predictive Control (FCS-MPC) strategy, originally developed for three-phase induction motors, can be effectively applied to five-phase induction motors. The implementation of FCS-MPC in five-phase systems has yielded promising results, confirming its capability to achieve precise control and stable performance under varying speed conditions.

For future work, further investigation into the impact of the x-y components, which are unique to five-phase induction motors, could help minimize losses and enhance the control strategy. Additionally, extending predictive control techniques to account for fault conditions in five-phase systems would enable full exploitation of their inherent advantages, improving performance and reliability across various industrial applications.

Appendix

Table. I
Five-phase induction motor parameters

Parameter	Value	Parameter	Value
P_{nom}[KW]	3.5	T_{nom}[N.m.]	12.7
$R_s[\Omega]$	9.5	$R_r[\Omega]$	7.3
L_s[H]	1.389	L_r[H]	1.331
L_m[H]	1.323	Pole pair number	1

References

[1] S. A. Gaikwad and S. M. Shinde, “Review on Five-phase Induction Motor fed by Five-phase Voltage Source Inverter with different Conduction Mode,” in *2020 International Conference on Industry 4.0 Technology (I4Tech)*, Pune, India, 2020, pp. 199–202, doi: 10.1109/I4Tech48345.2020.9102695.

[2] M. J. Duran and F. Barrero, "Recent Advances in the Design, Modeling, and Control of Multiphase Machines—Part II," *IEEE Trans. Ind. Electron.*, vol. 63, no. 1, pp. 459–468, Jan. 2016, doi: 10.1109/TIE.2015.2448211.

[3] K. Iffouzar et *al.*, "Improved direct field oriented control of multiphase induction motor used in hybrid electric vehicle application," *Int. J. Hydrogen Energy*, vol. 42, pp. 19296–19308, 2017.

[4] J. Kellner, S. Kaščák, and Ž. Ferková, "Investigation of the Properties of a Five-Phase Induction Motor in the Introduction of New Fault-Tolerant Control," *Appl. Sci.*, vol. 12, no. 4, p. 2249, 2022, doi: 10.3390/app12042249.

[5] G. Kulandaivel et *al.*, "Five-phase induction motor drive—A comprehensive review," *Front. Energy Res.*, vol. 11, p. 1178169, 2023, doi: 10.3389/fenrg.2023.1178169.

[6] L. Parsa, "On advantages of multi-phase machines," in *Proc. IEEE Ind. Electron. Conf. (IECON)*, Raleigh, NC, USA, 2005, pp. 6, doi: 10.1109/IECON.2005.1569139.

[7] M. Bermudez et *al.*, "Open-Phase Fault-Tolerant Direct Torque Control Technique for Five-Phase Induction Motor Drives," *IEEE Trans. Ind. Electron.*, vol. 64, no. 2, pp. 902–911, Feb. 2017, doi: 10.1109/TIE.2016.2610941.

[8] B. Chikondra, U. R. Muduli, and R. K. Behera, "An Improved Open-Phase Fault-Tolerant DTC Technique for Five-Phase Induction Motor Drive Based on Virtual Vectors Assessment," *IEEE Trans. Ind. Electron.*, vol. 68, no. 6, pp. 4598–4609, June 2021, doi: 10.1109/TIE.2020.2992018.

[9] B. S. Khaldi et *al.*, "DTC-SVM Sensorless Control of Five-Phase Induction Motor Based on Two Different Rotor Speed Estimation Approaches," *Nonlinear Dyn. Syst. Theory*, vol. 21, pp. 262–279, 2021.

[10] L. Vancini et *al.*, "Fault-Tolerant Control Strategies of Five-Phase Induction Motor Drives under Open-Switch Fault," in *Proc. Int. Conf. Electr. Mach. (ICEM)*, Valencia, Spain, 2022, pp. 1274–1280, doi: 10.1109/ICEM51905.2022.9910786.

[11] S. C. Rangari, H. M. Suryawanshi, and M. Renge, "New Fault-Tolerant Control Strategy of Five-Phase Induction Motor with Four-Phase and Three-Phase Modes of Operation," *Electronics*, vol. 7, p. 159, 2018, doi: 10.3390/electronics7090159.

[12] H. Guzman, M. J. Duran, F. Barrero, B. Bogado, and S. Toral, "Speed control of five-phase induction motors with integrated open-phase fault operation using model-based predictive current control techniques," *IEEE Trans. Ind. Electron.*, vol. 61, no. 9, pp. 4474–4484, Sep. 2014, doi: 10.1109/TIE.2013.2289882.

[13] E. Levi et *al.*, "Multiphase induction motor drives—A technology status review," *IET Electr. Power Appl.*, vol. 1, pp. 489–516, 2007, doi: 10.1049/iet-epa:20060342.

[14] J. Listwan, "DTC-ST and DTC-SVM control of five-phase induction motor with MRASCC estimator," *Przegląd Elektrotechniczny*, vol. 1, pp. 254–258, 2016, doi: 10.15199/48.2016.11.61.

[15] S. K. Barik and K. K. Jaladi, "Five-Phase Induction Motor DTC-SVM Scheme with PI Controller and ANN Controller," *Procedia Technol.*, vol. 25, pp. 816–823, 2016, *Proc. RAEREST 2016*, doi: 10.1016/j.protcy.2016.08.184.

[16] S. A. Gaikwad and S. M. Shinde, "Five-Phase Induction Motor Modeling and Its Analysis Using MATLAB/Simulink," in *Smart Technologies for Energy, Environment and Sustainable Development*, M. L. Kolhe, S. B. Jaju, and P. M. Diagavane, Eds., Springer Proc. Energy, Springer, Singapore, 2022, doi: 10.1007/978-981-16-6875-3_52.

[17] K. S. Aher and A. G. Thosar, "Modeling and simulation of five-phase induction motor using MATLAB/Simulink," *Int. J. Eng. Res. Appl.*, vol. 6, pp. 1–8, 2016.

[18] A. A. Mekhilef, A. Benachour, E. M. Berkouk, and A. Dali, "FCS-MPC of a DMC-fed Induction Machine with Unity Input Power Factor Using Rotating Vectors," in *Proc. 21st Int. Symp. Power Electron. (Ee)*, Novi Sad, Serbia, 2021, pp. 1–6, doi: 10.1109/Ee53374.2021.9628355.

[19] A. Zeghlache, H. Mekki, M. F. Benkhoris, A. Djerioui, D. Ziane, and S. Zeghlache, "Robust fault-tolerant control of a five-phase permanent magnet synchronous motor under an open-circuit fault," *Appl. Sci.*, vol. 14, no. 12, p. 5190, 2024, doi: 10.3390/app14125190.

[20] M. Bermúdez, H. Guzmán, I. González-Prieto, F. Barrero, M. J. Durán, and X. Kestelyn, "Comparative study of DTC and RFOC methods for the open-phase fault operation of a 5-phase induction motor drive," in *Proc. 41st Annu. Conf. IEEE Ind. Electron. Soc. (IECON)*, Yokohama, Japan, Nov. 2015, pp. 2702–2707, doi: 10.1109/IECON.2015.7392509.

[21] C. S. Lim et *al.*, "Experimental evaluation of model predictive current control of a five-phase induction motor using all switching states," in *Proc. 15th Int. Power Electron. Motion Control Conf. (EPE/PEMC)*, Novi Sad, Serbia, 4-6 Sept. 2012, pp. LS1c.4-1–LS1c.4-7, doi: 10.1109/EPEPEMC.2012.6397394.

[22] C. S. Lim et *al.*, "FCS-MPC-Based Current Control of a Five-Phase Induction Motor and its Comparison with PI-PWM Control," *IEEE Trans. Ind. Electron.*, vol. 61, pp. 149–163, 2014, doi: 10.1109/TIE.2013.2248334.

[23] H. Guzman et *al.*, "Speed Control of Five-Phase Induction Motors With Integrated Open-Phase Fault Operation Using Model-Based Predictive Current Control Techniques," *IEEE Trans. Ind. Electron.*, vol. 61, pp. 4474–4484, 2014, doi: 10.1109/TIE.2013.2289882.

[24] C. Martín et *al.*, "Five-Phase Induction Motor Rotor Current Observer for Finite Control Set Model Predictive Control of Stator Current," *IEEE Trans. Ind. Electron.*, vol. 63, pp. 4527–4538, 2016, doi: 10.1109/TIE.2016.2536578.

[25] H. Guzman and A. Iqbal et *al.*, "Reduction of common-mode voltage using a simplified FCS-MPC for a five-phase induction motor drive," *J. Eng.*, 2019, doi: 10.1049/joe.2018.8045.